0013-7227/06/$15.00/0
Printed in U.S.A.

Endocrinology 147(12):5662–5675

doi: 10.1210/en.2006-0916

Gene Expression Profiling of Human Endometrial-Trophoblast Interaction in a Coculture Model

Roxana M. Popovici, Nina K. Betzler, Miriam S. Krause, Man Luo, Julia Jauckus, Ariane Germeyer, Sandra Bloethner, Andreas Schlotterer, Rajiv Kumar, Thomas Strowitzki, and Michael von Wolff

Department of Gynecological Endocrinology and Reproductive Medicine (R.M.P., N.K.B., M.S.K., M.L., J.J., A.G., T.S., M.v.W.), University of Heidelberg, 69115 Heidelberg, Germany; Division of Molecular Genetic Epidemiology (S.B., R.K.), German Cancer Research Center, and Division of Endocrinology and Metabolism (A.S.), Department of Medicine, University of Heidelberg, 69120 Heidelberg, Germany

Investigating the interaction of human endometrium and trophoblast during implantation is difficult *in vitro* and impossible *in vivo*. This study was designed to analyze the effect of trophoblast on endometrial stromal cells during implantation by comprehensive gene profiling. An *in vitro* coculture system of endometrial stromal cells with first-trimester trophoblast explants was established. Trophoblast and endometrial stromal cells were separated after 24 h. Gene expression of endometrial stromal cells after coculture was compared with the gene expression of endometrial stromal cells cultured alone by microarray analysis. We confirmed the expression of distinct genes using real-time PCR. Genes up-regulated included those for inflammatory response, immune response, and chemotaxis (pentraxin-related gene 3, chemokine ligands, IL-8, IL-1 receptors, IL-18 receptor, IL-15, IL-15 receptor, TNF-α-induced protein 6, and IL-6 signal transducer), regulators of cell growth (IGF-binding proteins 1 and 2) and signal transduction. Also up-regulated were genes for growth and development, glucose metabolism, and lipid metabolism: DKK-1, WISP, IGF-II, hydroxysteroid 11β-dehydrogenase 1, hydroxyprostaglandin dehydrogenase 15, prostaglandin E synthase, prostaglandin F receptor, aldehyde dehydrogenase 1 family, member A3 and phosphatidic acid phosphatase type 2B. Other genes included genes for cell-cell signaling (pre-B-cell colony-enhancing factor 1), proteolysis, calcium ion binding, regulation of transcription, and others. Down-regulated genes included genes for proteolysis (MMP-11 and mitochondrial intermediate peptidase), genes for cell death (caspase 6, death-associated protein kinase 1, and histone deacetylase 5), transcription factors (sex determining region Y-box 4, dachshund homolog 1, ets variant gene 1, and zinc finger protein 84 and 435), and genes for humoral immune response (CD24 antigen). Trophoblast has a significant impact on endometrial stromal cell gene expression. Some of the genes regulated by trophoblast in endometrial stromal cells are already known to be regulated by progesterone and show the endocrine function of trophoblast during pregnancy. Others are genes so far unknown to play a role in endometrial-trophoblast interaction and open a wide field of investigation. (*Endocrinology* 147: 5662–5675, 2006)

DESPITE THE POSSIBILITY of extracorporal fertilization and extensive new technology, the process of implantation and the interaction between maternal endometrium and invading trophoblast are even today difficult to explore. Hence, the search for better understanding of this process continues and is transferred into the *in vitro* setting (1–3). After coming into contact with the maternal decidua, cytotrophoblast cells proliferate and form columns of invasive cytotrophoblast cells, also known as the extravillous trophoblast (4). These cells invade into the decidualized endometrial stromal compartment and the inner third of the myometrium and thus anchor the pregnancy inside the uterus. They also provide the conceptus with nourishment by invading into the maternal vessels (5). Contrary to cancer cells, these invasive properties are well regulated and confined in time and space (6). Only first- and early second-trimester trophoblast has the capacity to invade; later on, the trophoblast only proliferates and increases in size (6). In the first trimester, cells migrate through the decidua; later on, the remodeling of the inner myometrial portion occurs at 14–18 wk gestation and is mediated by intravascular migration of extravillous trophoblast cells (4). Invasion is mediated by multiple factors such as matrix metalloproteinases (MMPs) and other collagenases (7, 8). In abnormalities such as preeclampsia, trophoblast invasion of the uterine spiral arteries does not proceed beyond the decidual portion of the spiral arteries (9, 10); on the other side, when trophoblast invasion becomes excessive, placenta accreta results (11).

Hence, invasion of the trophoblast is a very complex process, and multiple factors must necessarily regulate differentiation, proliferation, and invasion of trophoblast cells. The maternal endometrium is equipped with different cell populations that help to regulate these processes. Endometrial epithelial cells, endometrial stromal cells, immune cells in the endometrium as well as vascular endothelial cells, and, later on in pregnancy, myometrial cells all come into contact with trophoblast. Endometrial stromal cells play a major role during the interaction with the invading trophoblast and change their morphology and secretory pattern during the secretory phase of the cycle in preparation for the invasion. This study was therefore designed to evaluate *in vitro* the interaction between endometrial stromal cells and trophoblast explants.

First Published Online August 31, 2006

Abbreviations: DAPI, 4′,6-Diamidino-2-phenylindole; GCOS, GeneChip operating software; GO, gene ontology; GOTM, GO tree machine.

***Endocrinology* is published monthly by The Endocrine Society (http://www.endo-society.org), the foremost professional society serving the endocrine community.**

TABLE 1. Primers used for microarray gene expression validation

Gene	Forward primer 5′–3′	Reverse primer 5′–3′	Size (bp)
TIMP3	TGAACTATCGGTATCACCTG	TTCTTGTTGCAGTTTGGCAG	190
DKK-1	GGGAATTACTGCAAAAATGGAATA	ATGACCGGAGACAAACAGAAC	190
IGFBP-1	CTATGATGGCTCGAAGGCTC	TTCTTGTTGCAGTTTGGCAG	156
PTX3	CATCCAGTGAGACCAATGAG	GTAGCCGCCAGTTCACCATT	287
IL-8	ATCACTTCCAAGCTGGCCGTGGCT	TCTCAGCCCTCTTCAAAAACTTCTC	288
MMP-11	CTTCCGAGGCAGGGACTACT	AGAAGTCAGGACCCACGAGA	227
SOX4	TGAGTTCGCGACACTATGTA	GTGCCTGTCATGTTATATTA	240
FGF-1	CAACGGGGGCCACTTCTT	CAGCTCCCGTTCTTCTTG	300
RPL19	GTAAGCGGAAGGGTACAGCCA	TTGTCTGCCTTCAGCTTGTG	211

Materials and Methods

Patients and samples

Endometrial biopsies were obtained from women undergoing diagnostic hysteroscopy at the Women's University Hospital, Heidelberg (n = 10), during the proliferative phase (d 8–12) for reasons of uterine myoma (60%) or septal uterus (40%). Patients had a regular cycle without hormonal treatment and no suspect of malignancy. Average age was 33 ± 4 yr. Trophoblast tissue was obtained from legal early pregnancy terminations of uncomplicated, unwanted pregnancies (n = 10). Median age was 24 ± 5 yr. All samples were obtained after informed consent, and the protocol was approved by the University of Heidelberg Ethics Committee.

Establishment of cocultures

Endometrial stromal cells were isolated by a protocol previously published (12) from 10 different patients. Trophoblast tissue (n = 10) was isolated by mechanical dissection and washed thoroughly with warm PBS, and approximately 25 trophoblast explants of an average of 3 mm were carefully set on confluent stromal cells in a 4 cm diameter culture dish. Most trophoblast explants attached to stromal cells after approximately 2 to 3 h and coculture was incubated for a total of 24 h. Stromal cell monocultures from the same patient were used as controls. After 24 h, trophoblast explants were carefully removed from stromal cells with sterile tweezers under the microscope. All stromal cells used were from proliferative-phase endometrium and had been passaged once in culture. Trophoblast explants were taken from placentas at 6–8 wk of pregnancy.

Immunofluorescence

To ascertain that the trophoblast was close to totally removed from stromal cells, immunofluorescent staining of stromal cells before and after separation was performed in preliminary experiments (see Fig. 1). Briefly, cocultures (n = 4) were visualized under a microscope and photographed using a digital camera. After three washings with PBS, cocultures before and after separation with tweezers were fixed with ice-cold 80% methanol for 10 min, air dried, and stored at −80 C. For immunofluorescent staining, nonspecific background was blocked with solution A of the Histostain-Plus Kit (Zymed Laboratories, San Francisco, CA), and samples were then incubated with primary antibodies, monoclonal mouse-antihuman vimentin for stromal cells (1:50; Dako, Copenhagen, Denmark) and monoclonal mouse-antihuman cytokeratin-7 for cytotrophoblast cells (1:50; Dako) for 1 h at room temperature (21 C), respectively. After three careful washings with PBS and incubation with a goat-antimouse fluorescein-isothiocyanate-conjugated secondary antibody (1:100; Dako) for 1 h at 4 C, slides were washed in distilled water and covered with Vectashield plus 4′,6-diamidino-2-phenylindole (DAPI) mounting medium (Vector, Burlingame, CA).

RNA isolation

RNA (n = 6; three experiments for microchip analysis and another three experiments for real-time PCR) was isolated from stromal cells after trophoblast coculture as well as from controls using Trizol (Invitrogen, Carlsbad, CA) according to the manufacturer's instructions. Total RNA was then subjected to a cleanup using RNeasy Mini Kit (QIAGEN, Hilden, Germany). RNA concentration was measured by UV spectrophotometry, and OD 260/280-nm ratios between 1.9 and 2.1 were obtained for all RNA samples. The integrity of total RNA isolated from stromal cells was determined on the Bioanalyzer 2100 System (Agilent Technologies, Palo Alto, CA) using 400 ng RNA from each sample.

Gene expression profiling

A total of three experimental sets made up of stromal cells after coculture and stromal cells without previous coculture were used for microarray analysis. Two micrograms of total RNA from each sample were converted into double-stranded cDNA using SuperScript Double-Stranded cDNA Synthesis Kit (Invitrogen) according to the manufacturer's protocol. Double-stranded cDNA was cleaned up with the GeneChip Sample Cleanup Module (Affymetrix, Sunnyvale, CA).

Twelve microliters of the purified cDNA were used for the synthesis of biotin-labeled cRNA using ENZO Labeling Kit (ENZO Diagnostics, Farmingdale, NY). Each cRNA was fragmented according to the protocol in the Affymetrix GeneChip Expression Analysis manual, with quality assessed by hybridization of a 5-μg aliquot to a test chip (TestChip3; Affymetrix). Only cRNA samples that showed at least 27% present calls and 3′ to 5′ signal ratios of 0.9–1.5 for the housekeeping genes β-actin and RPL on the test arrays were hybridized to Human HG-U133A 2.0 microarray chips (Affymetrix) with 22,277 probe sets, representing 14,500 human genes (the list of genes is available at www.affymetrix.com). Ten micrograms (0.05 μg/μl) of fragment-labeled cRNA was hybridized onto the array at 45 C for 16 h. Hybridization, washing (on GeneChip Fluidics Station 400; Affymetrix) and scanning (with GeneArray Scanner; Affymetrix) were performed at the German Cancer Research Centre, Heidelberg, Germany, according to the manufacturer's (Affymetrix) instructions. Complete transcription and hybridization were validated using bacterial sequences as external control as well as several housekeeping genes as internal controls.

Data analysis

Image analysis. Image analysis was performed with Affymetrix GeneChip operating software (GCOS) to analyze scanned images, to convert intensities to a numerical format, and to obtain a detection call. Target intensities of microarray images were scaled to an average hybridization intensity of 100 to normalize signals between individual chips. Detection call indicated whether a transcript was reliably detected (present) or below background levels (absent). Probe sets whose hybridization sig-

TABLE 2. Annealing and extension temperature and time for real-time PCR

Primer	Annealing temperature (C)	Annealing time (sec)	Extension temperature (C)	Extension time (sec)
IL-8	69	10	72	13
PTX3	56	10	72	13
IGFBP-1	55	10	72	8
DKK-1	58	10	72	9
TIMP3	55	10	72	10
MMP-11	55	10	72	10
SOX4	51	10	72	11
FGF-1	52	10	72	13
RPL19	58	10	72	10

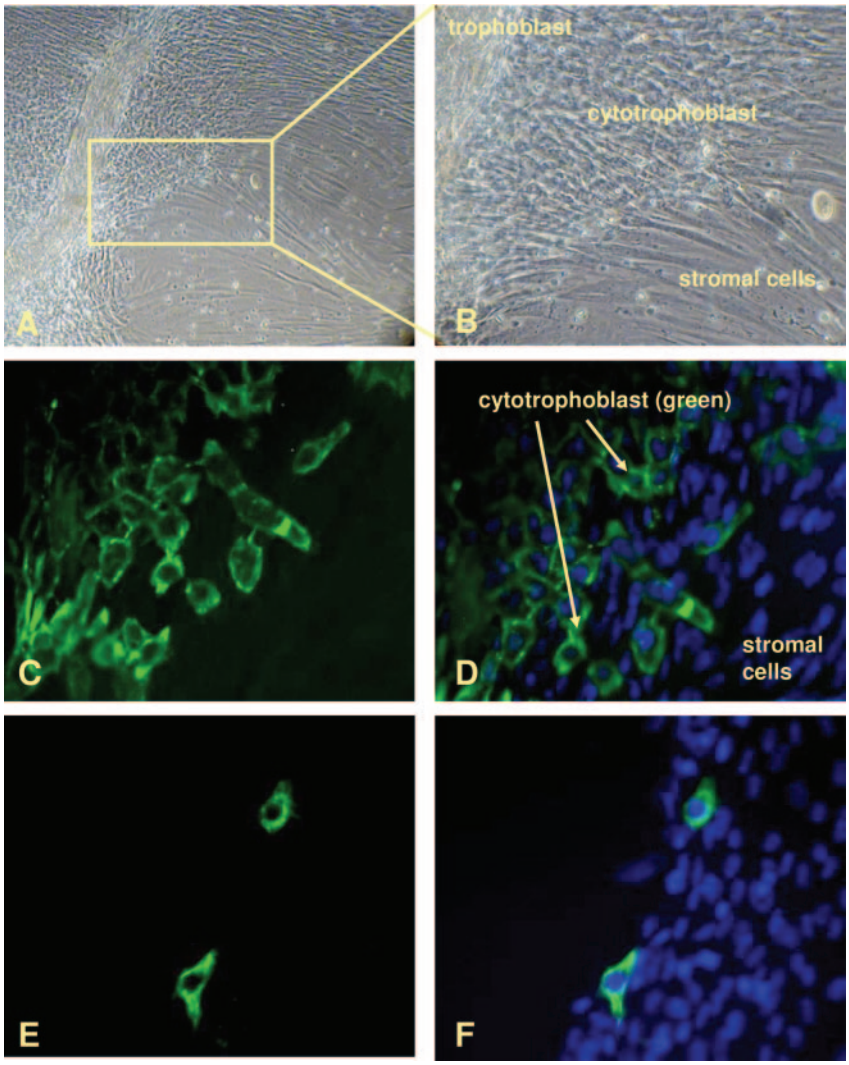

FIG. 1. Endometrial stromal cells cocultured with trophoblast before and after removal of trophoblast explant. Trophoblast explants were cocultured with endometrial stromal cells for 24 h and then removed with sterile tweezers under the microscope. Cell cultures were stained with cytokeratin-7 and DAPI before and after removal of trophoblast to check for cytotrophoblast cells. A, Trophoblast explant, budding cytotrophoblast, and stromal cells in low magnification (×200); B, higher magnification (×400) from A; C and D, cytotrophoblast stained with specific antibody for cytokeratin-7 (*green*) and counterstaining for all nuclei with DAPI (*blue*) before trophoblast removal; E and F, cytokeratin-7-specific immunofluorescent staining of the few remaining cytotrophoblast cells after careful removal of trophoblast branches. The remaining counterstained nuclei are from stromal cells.

nals were below background level, *i.e.* called absent, were not included. A detection *P* value, which is calculated using the one-sided Wilcoxon's signed rank test, reflects the confidence of the detection call. Additionally, a signal value was calculated for each probe set on the array using the one-step Tukey's biweight estimate, which assigns a relative measure of abundance to the transcript (signals).

Pairwise comparison. GCOS was used for pairwise comparisons of expression profiles between stromal cells after coculture with trophoblast (designated experimental arrays) and stromal cells that had not been in coculture (designated as baseline arrays). During comparison analysis, each probe set on the experimental array was compared with its counterpart on the baseline array, and a change in *P* value was calculated indicating the change call: increase, marginal increase, decrease, marginal decrease, or no change in gene expression. A second algorithm was used to calculate a quantitative estimate of the gene expression change in the form of signal log ratio. A signal log ratio of 1 or −1 corresponded to an increase or decrease, respectively, in transcript level by 2-fold. Thus, from the three experiments, a total of nine comparisons (stroma only *vs.* stroma after coculture) were made, and the obtained signal log ratios were averaged and then translated into a fold change number. Additional analysis that included sorting of data and identification of overlaps between changed probes was done by using Data Mining Tool software (Affymetrix). Comparisons with a no change call were removed. Gene expression data were sorted according to the relative change and fold change values, and for identification of differentially expressed genes and data interpretation, probe sets with a fold change greater than or equal to 2 were used. Because the data were not normally distributed, nonparametric testing was conducted using Mann-Whitney *U* test to calculate the *P* values, applying $P \leq 0.05$ to assign statistical significance between the two groups.

Identification of genes. For gene identification and annotation, we applied our results to Netaffx Analysis Center (http://www.affymetrix.com/analysis/index.affx), which maps the Affymetrix probe identifiers to gene identities including links to Gene Ontology and Pathway software.

Gene ontology (GO) classification. GO tree machine (GOTM) is a web-based tool that was used to generate groups of genes from the genes identified by pairwise comparisons to be up- or down-regulated. GOTM uses GO hierarchies to discover significant biological processes, molecular functions, and cellular components in a gene list.

Ingenuity Pathways Analysis. A data set containing gene identifiers and corresponding expression values was uploaded into the Ingenuity Pathways application. Each gene identifier was mapped to its corresponding gene object in the Ingenuity Pathways Knowledge Base. A 2-fold change was set to identify genes whose expression was significantly differentially regulated. These genes, called focus genes, were overlaid onto a global molecular network developed from information contained in the Ingenuity Pathways Knowledge Base. Networks of these focus genes were then algorithmically generated based on their connectivity.

The molecular relationship between genes is shown in a graphical representation. Genes or gene products are represented as nodes, and the biological relationship between two nodes is represented as an edge

TABLE 3. Genes up-regulated in human endometrial stromal cells after trophoblast coculture

Gene symbol	Fold change up	Gene ID	Description
Cytokines inflammatory response/chemotaxis			
IL-8	367.0	211506_s_at	IL-8
CXCL2	291.0	209774_x_at	Chemokine (C-X-C motif) ligand 2
CXCL1	195.0	204470_at	Chemokine (C-X-C motif) ligand 1 (melanoma growth-stimulating activity, α)
PTX3	105.0	206157_at	Pentraxin-related gene, rapidly induced by IL-1β
CCL2	103.0	216598_s_at	Chemokine (C-C motif) ligand 2
CXCL6	83.0	206336_at	Chemokine (C-X-C motif) ligand 6 (granulocyte chemotactic protein 2)
CCL8	30.0	214038_at	Chemokine (C-C motif) ligand 8
IL-1BR1	13.0	206618_at	IL-2 18 receptor 1
IL-15	10.0	217371_s_at	IL-15
IL-7R	8.0	205798_at	IL-7 receptor, regulation of
IL-15RA	4.5	207375_s_at	IL-15 receptor, α
CD1D	4.5	205789_at	CD1D antigen, d polypeptide
PROCR	2.5	203650_at	Protein C receptor, endothelial (EPCR)
IFI35	2.5	209417_s_at	Interferon-induced protein 35
IL-6 ST	2.4	204863_s_at	IL-6 signal transducer
F3	2.0	204363_at	Coagulation factor 3 (thromboplastin)
Lipid metabolism/steroid metabolism			
HSD11B1	84.3	205404_at	Hydroxysteroid 11β-dehydrogenase 1
HPGD	64.1	211549_s_at	Hydroxyprostaglandin dehydrogenase 15-(NAD)
STAR	14.0	204548_at	Steroidogenic acute regulator, C21
PPAP2B	4.6	209355_s_at	Phosphatidic acid phosphatase type 2B
UGCG	3.0	204881_s_at	UDP-glucose ceramide glucosyltransferase
MGLL	2.7	211026_s_at	Monoglyceride lipase
FADS1	2.5	208962_s_at	Fatty acid desaturase 1
HMGCS1	2.5	205822_s_at	3-Hydroxy-3-methylglutaryl-coenzyme A synthase 1 (soluble)
LSS	2.2	202245_at	Lanosterol synthase
FADS3	2.2	216080_s_at	Fatty acid desaturase 3
Transport molecules			
MAOA	25.6	204388_s_at	Monoamine oxidase A
MAOB	7.5	204041_at	Monoamine oxidase B, electron transport
SLC22A4	4.5	205896_at	Solute carrier family 22 (organic cation transporter), member 4
ZC3H12A	4.5	218810_at	Zinc finger CCCH-type containing 12A
SLC7A8	4.4	216603_at	Solute carrier family 7 (cationic amino acid transporter, y+ system), member 8
SLC39A8	4.1	219869_s_at	Solute carrier family 39 (zinc transporter), member 8
SLC39A14	4.0	212110_at	Solute carrier family 39 (zinc transporter), member 14
KCNJ8	3.4	205303_at	Potassium inwardly-rectifying channel, subfamily J, member 8
DPYD	3.0	204646_at	Dihydropyrimidine dehydrogenase
COL18A1	3.0	209081_s_at	Collagen, type XVIII, α1
ZFP36	2.9	201531_at	Zinc finger protein 36, C3H type, homolog
COL7A1	2.9	204136_at	Collagen, type VII, alpha 1
TAP1	2.4	202307_s_at	Transporter 1, ATP-binding cassette, sub-family B (MDR/TAP)
CYP51A1	2.4	216607_s_at	Cytochrome P450, family 51, subfamily A, polypeptide 1
SQLE	2.3	209218_at	Squalene epoxidase
CYB5	2.3	215726_s_at	Cytochrome b-5
RRAS	2.2	212647_at	Related RAS viral oncogene homolog
DMXL2	2.1	212820_at	Dmx-like 2
Signal transduction			
CGA	82.3	204637_at	Glycoprotein hormones, α polypeptide
SNX10	5.4	218404_at	Sorting nexin 10
PBEF1	5.4	217738_at	Pre-B-cell colony enhancing factor 1
ADORA2B	5.0	205891_at	Adenosine A2b receptor
IL15RA	4.5	207375_s_at	IL-15 receptor, α
GPR126	4.4	213094_at	G protein-coupled receptor 126
TGM2	3.9	211003_x_at	Transglutaminase 2 (C polypeptide, protein-glutamine-γ-glutamyltransferase)
EDG2	3.4	204037_at	Endothelial differentiation, lysophosphatidic acid G-protein-coupled receptor, 2
ADRA2C	2.7	206128_at	Adrenergic, α2C-, receptor
RGC32	2.7	218723_s_at	Regulation of cyclin dependent protein kinase activity response gene to complement 32
OSMR	2.5	205729_at	Oncostatin M receptor
TRAF3IP2	2.4	215411_s_at	TRAF3 interacting protein 2
GPRC5B	2.3	203632_s_at	G protein-coupled receptor, family C, group 5, member B

Table continues on next page.

TABLE 3. *Continued*

Gene symbol	Fold change up	Gene ID	Description
TRIB	2.3	202241_at	Tribbles homolog 1 (*Drosophila*)
RASSF4	2.1	49306_at	Ras association domain factor
IFNGR1	2.0	211676_s_at	Interferon-γ receptor 1
Proteolysis			
MMP12	26.0	204580_at	Matrix metallopeptidase 12 (macrophage elastase)
ADAMTS3	5.4	214913_at	ADAM metallopeptidase with thrombospondin type 1 motif, 3
TIMP3	4.5	201147_s_at	TIMP metallopeptidase inhibitor 3 (Sorsby fundus dystrophy, pseudoinflammatory)
ABLIM3	4.3	205730_s_at	Actin binding LIM protein family, member 3
PAPPA	4.1	201981_at	Pregnancy-associated plasma protein A, pappalysin 1
CTSS	3.8	202901_x_at	Cathepsin S
CPM	3.4	206100_at	Carboxypeptidase M
ADAMTS1	3.0	222162_s_at	ADAM metallopeptidase with thrombospondin type 1 motif, 1
PSMB9	2.9	204279_at	Proteasome (prosome, macropain) subunit, β-type, 9 (large multifunctional peptidase 2)
HGF	2.4	209960_at	Hepatocyte growth factor (hepapoietin A; scatter factor)
MMD	2.4	203414_at	Monocyte to macrophage differentiation
ABHD5	2.3	218739_at	Abhydrolase domain containing 5
MME	2.3	203435_s_at	Membrane metallo-endopeptidase (neutral endopeptidase, enkephalinase, CALLA, CD10
PSMB10	2.2	202659_at	Proteasome (prosome, macropain) subunit, beta type, 10
Angiogenesis			
S100P	37.0	204351_at	S100 calcium-binding protein P
TNFAIP2	3.8	202510_s_at	TNFα-induced protein 2
NRP1	2.0	212298_at	Neuropilin 1
Development			
DKK1	7.1	204602_at	Dickkopf homolog 1 (*Xenopus laevis*)
EMP2	3.1	204975_at	Epithelial membrane protein 2
IGFBP4	2.1	201508_at	IGF-binding protein 4
TAGLN2	2.0	200916_at	Transgelin 2
PDPN	2.0	221898_at	Podoplanin
Ion binding/detoxification			
MT1M	19.0	217546_at	Metallothionein 1M
MT1X	6.0	208581_x_at	Metallothionein 1X
MT1H	6.0	206461_x_at	Metallothionein 1H
MT1F	5.0	213629_x_at	Metallothionein 1F (functional)
MT1G	4.0	204745_x_at	Metallothionein 1G
MT2A	4.0	212185_x_at	Metallothionein 2A
MT1E	4.0	212859_x_at	Metallothionein 1E (functional)
Apoptosis			
TNFAIP3	18.0	202643_s_at	TNFα-induced protein 3
NFKBIA	6.0	201502_s_at	Nuclear factor of κ-light polypeptide gene enhancer in B-cells inhibitor
TNFAIP6	4.4	206026_s_at	TNFα-induced protein 6
TNFAIP8	2.3	210260_s_at	TNFα-induced protein 8
PDCD5	2.1	219275_at	Programmed cell death 5
Cell growth/cell cycle			
IGFBP1	12.0	205302_at	IGF-binding protein 1
SPP1	6.5	209875_s_at	Secreted phosphoprotein 1 (osteopontin)
IGFBP2	4.4	202718_at	IGF-binding protein 2
BCL3	3.6	204908_s_at	B-cell CLL/lymphoma 3
IGF2	2.9	202410_x_at	IGF-2 (somatomedin A)
EFEMP1	2.6	201842_s_at	EGF-containing fibulin-like extracellular matrix protein 1
STAT1	2.4	209969_s_at	Signal transducer and activator of transcription 1, 91 kDa
IGFBP4	2.1	201508_at	IGF-binding protein 4
EGFR	2.0	201983_s_at	Epidermal growth factor receptor
Transcription			
CEBPD	12.1	213006_at	CCAAT/enhancer binding protein (C/EBP), δ
GCM1	10.0	206269_at	Glial cells missing homolog 1 (Drosophila)
MYC	6.3	202431_s_at	v-*myc* Myelocytomatosis viral oncogene homolog (avian)
GATA3	6.1	209604_s_at	GATA binding protein 3
NFIB	4.6	209290_s_at	Nuclear factor I/B
ELL2	3.7	214446_at	Elongation factor, RNA polymerase II, 2
JUNB	3.6	201473_at	Jun B protooncogene
RELB	3.2	205205_at	v-*rel* Reticuloendotheliosis viral oncogene homolog B)
NFIL3	3.2	203574_at	Nuclear factor, IL-3 regulated
NPAS2	2.7	39549_at	Neuronal PAS domain protein 2
NFKB2	2.2	207535_s_at	Nuclear factor of κ-light polypeptide gene enhancer in B-cells 2 (p49/p100)

TABLE 3. *Continued*

Gene symbol	Fold change up	Gene ID	Description
Response to oxidative stress			
SOD2	31.0	216841_s_at	Superoxide dismutase 2, mitochondrial
GPX3	18.1	214091_s_at	Glutathione peroxidase 3 (plasma)
PDLIM1	2.3	208690_s_at	PDZ and LIM domain 1 (elfin)
Prostaglandin metabolism			
PTGES	11.0	210367_s_at	Prostaglandin E synthase
Protein metabolism			
GCH1	10.8	204224_s_at	GTP cyclohydrolase 1
MAP3K8	6.6	205027_s_at	MAPK 8
SLC7A8	5.2	216604_s_at	Solute carrier family 7, amino acid 8
LEPREL1	3.3	218717_s_at	Protein metabolism, leprecan-like 1
LDLR	2.9	202067_s_at	Low-density lipoprotein receptor
LYN	2.8	202626_s_at	v-*yes*-1 Yamaguchi sarcoma viral related oncogene homolog
FAH	2.8	202862_at	Fumarylacetoacetate hydrolase
PPIF	2.2	201489_at	Peptidylprolyl isomerase F (cyclophilin F)
GCLM	2.1	203925_at	Glutamate-cysteine-ligase subunit
TAPBP	2.0	208829_at	TAP binding protein (tapasin)
Carbohydrate metabolism			
CA2	11.0	209301_at	Carbonic anhydrase II
CA12	5.3	203963_at	Carbonic anhydrase XII
CHST11	3.1	219634_at	Carbohydrate (chondroltin 4) sulfotransferase 11
IRS2	3.0	209185_s_at	Insulin receptor substrate 2
CHST2	2.8	203921_at	Carbohydrate (*N*-acetylglucosamine-6-O) sulfotransferase 2
ALDH2	2.4	201425_at	Aldehyde dehydrogenase 2 family
INSIG1	2.3	201625_s_at	Insulin-induced gene 1
Cell adhesion			
CD47	2.3	211075_s_at	CD47 antigen
ITGA5	2.0	201389_at	Integrin, α5
Others			
LAIR2	109.1	207509_s_at	Leukocyte-associated Ig-like receptor 2
KYNU	43.9	217388_s_at	Kynureninase (L-kynurenine hydrolase)
MGC5618	9.2	221477_s_at	Hypothetical protein MGC5618
CHST7	6.9	206756_at	Carbohydrate (*N*-acetylglucosamine 6-O) sulfotransferase 7
NNMT	6.9	202238_s_at	Nicotinamide *N*-methyltransferase
TFPI2	5.8	209278_s_at	Tissue factor pathway inhibitor 2
LOC440737	5.2	211456_x_at	Similar to 60S-ribosomal protein L35
S100A3	5.0	206027_at	S100 calcium-binding protein A3
LCP1	4.1	208885_at	Lymphocyte cytosolic protein 1 (L-plastin)
SQRDL	3.8	217995_at	Sulfide quinone reductase like (yeast)
C1orf10	3.7	209183_s_at	Chromosome 10 open reading frame 10
FLJ20701	3.4	219093_at	Hypothetical protein FLJ 20701
FLJ23191	3.3	219747_at	Hypothetical protein FLJ 23191
C14orf147	3.2	213508_at	Chromosome 14 open reading frame 147
CRISPLD2	3.2	221541_at	Cysteine-rich secretory protein
POPDC3	3.2	219926_at	Popeye domain containing 3
SAT	3.2	213988_s_at	Spermine *N*1-acetyltransferase
VTAP	2.8	210285_x_at	Wilms tumor 1 associated protein
LOC492304	2.5	202409_at	Putative insulin-like GF2-associated protein
LHFP	2.4	218656_s_at	Lipoma HMGIC fusion partner
LDH A	2.3	200650_s_at	Lactate dehydrogenase A
GLUL	2.2	217202_s_at	Glutamate-ammonia ligase
ADA	2.1	204639_at	Adenosine deaminase
UCK2	2.0	209825_s_at	Uridine-cytidine-kinase 2
PHLDA2	2.0	209803_s_at	Pleckstrin homology-like domain
LOC283824	2.0	213725_x_at	Hypothetical protein LOC283824
OAS3	2.0	218400_at	2′-5′-Oligoadenylate synthetase 3
NP	2.0	201695_s_at	Nucleoside phosphorylase

The fold change is derived from pairwise comparisons of average signal log ratios from three experiments (nine comparisons, at least eight of which had to show a signal log ratio of +1, equivalent to a 2-fold up-regulation).

(line). All edges are supported by at least one reference from the literature, from a textbook, or from canonical information stored in the Ingenuity Pathways Knowledge Base. Human, mouse, and rat orthologs of a gene are stored as separate objects in the Ingenuity Pathways Knowledge Base but are represented as a single node in the network. The intensity of the node color indicates the degree of up-regulation (*red*) or down-regulation (*green*). Nodes are displayed using various shapes that represent the functional class of the gene product.

Validation of gene expression data

Real-time PCR. Gene expression of certain genes that were regulated in the array experiment was determined by quantitative real-time PCR in a fluorescent temperature cycler (LightCycler; Roche Diagnostics, Berkeley, CA) according to the manufacturer's instructions, using the oligonucleotide primer pairs shown in Table 1. Total RNA that had been used for the chip hybridization (n = 3) and additional total RNA from three

new experiments (total n = 6) was isolated using the RNeasy Mini Kit (QIAGEN), and 1 μg total RNA was reverse transcribed using the First-Strand cDNA Synthesis Kit for RT-PCR (Roche Diagnostics). One tenth of each reverse transcriptase reaction was amplified in a PCR tube containing 3 mM (IL-8, MMP-11, and RPL-19), 4 mM (TIMP-3, FGF-1, PTX-3, and IGFBP-1), or 5 mM (SOX4 and DKK-1) $MgCl_2$, 0.5 μM of each primer and 1× LightCycler FastStart DNA Master SYBR Green I mix (Roche Diagnostics). After an initial preincubation step of 10 min at 95 C, the amplification process, consisting of 40 PCR cycles, was performed. Each cycle consisted of 95 C for 10 sec as denaturation phase, followed by primer annealing and extension (Table 2).

SYBR Green I fluorescence was monitored after each cycle. Levels of mRNA expression were quantified by using the second-derivative maximum method of the LightCycler Software (Roche Diagnostics) and were normalized to RPL19. Amplification of specific transcripts was confirmed by melting curve profiles at the end of each PCR.

Statistical analysis of PCR data. All variables were tested in six culture experiments (stroma cells only *vs.* stromal cells after coculture; n = 6). Data were analyzed by ANOVA using the Stat-View software (Abacus Concepts, Berkeley, CA). Significance between groups was determined using Fisher's protected least significant difference *post hoc* test, with $P < 0.05$ considered significant, $P < 0.01$ highly significant, and $P < 0.001$ extremely highly significant. Results are shown as fold change ± SEM on a $\log_{10}$ scale.

Results

Cell culture and immunofluorescence

Cell cultures were established as described in *Materials and Methods*. Stromal cells that had been cultured together with trophoblast explants for 24 h (and from which trophoblast explants were then removed) were compared with stromal cells from the same patient that were cultured without trophoblast. Trophoblast explants were removed carefully without leaving significant cytotrophoblast cells in contact with stromal cells before RNA isolation. This was ascertained by immunofluorescent staining of cocultures before and after trophoblast removal in preliminary experiments (Fig. 1). Exemplary light microscopy of a trophoblast explant on stromal cells is shown in panels A and B. C and D show immunofluorescence of cytokeratin-7-stained trophoblast in coculture. Panels E and F show trophoblast staining by cytokeratin-7 (*green* staining) after removal of trophoblast. The DAPI-stained (*blue* stain) cells in panel F are stromal cells (with exception of the two cytokeratin-7-positive cytotrophoblast cells). For the microarray experiments, three experimental groups were selected.

Data analysis

Expression analysis using the GCOS module showed an average of 58.93% (13,130 ± 411) of transcripts were scored as being present in stromal cells without coculture and an average of 57.63% (12,833 ± 383) of transcripts were present in stromal cells after coculture. Pairwise comparison was performed, and we thus received nine data sets from the three experimental setups. Two criteria were applied for sorting the data in Data Mining Tool. First, change of expression level of 2-fold or more (which is equal to a signal log ratio of at least 1 or −1, respectively) and, second, 88–100% concordance in increase or decrease of expression in each single comparison (from three different experiments from which a total of nine comparisons were made, a change had to be seen in at least eight of these nine comparisons, *i.e.* 88%). Gene expression changes identified by these criteria were then tested further by Mann-Whitney *U* test applying $P < 0.05$ to show statistical significance between the two groups. Based on these criteria, expression of 165 genes was increased (Table 3) in stromal cells after coculture with trophoblast *vs.* stromal cells that had not been cultured with trophoblast, and expression of 119 genes was decreased (Table 4).

The data received by this stringent filtering and analysis was then imported into GOTM, which allowed grouping of genes into different categories (Tables 3 and 4). In stromal cells that had been in contact with trophoblast, genes involved in inflammatory response and signal transduction were most markedly up-regulated. In order of maximal fold change (Table 3), these include IL-8, chemokine ligand 1 and 2 (CXCL1 and 2), pentraxin-related gene (PTX3), and IL-1 receptor type 1 and type 2 (IL1R1 and IL1R2) as well as glycoprotein hormone α-polypeptide (CGA), G protein-coupled receptor 126 (GPR126), and IL-15 receptor α (IL-15RA). Further up-regulated were genes involved in proteolysis such as MMP-12, ADAM metallopeptidase type 1 motif 1 and 3 (ADAMTS1 and ADAMTS3), and the proteolysis inhibitor TIMP3. Additional genes were up-regulated, including apoptotic genes like TNF-α-induced protein 3 and 6 (TNFAIP3 and TNFAIP6) as well as cell-growth-related genes like IGFBP-1, IGFBP-2, IGFBP-4, osteopontin, and IGF-2. Genes in response to reactive oxygen species and oxidative stress, *e.g.* superoxide dismutase 2 (SOD2) or glutathione peroxidase 3 (GPX3) were also up-regulated. Genes responsible for transport, be it metal ion (metallothionein 2A, MT2A, and solute carrier family 39 zinc transporter, SLC39), sodium ion (solute carrier family 22, SLC22), or electron (monoamine oxidase A and B, MAO A and MAO B) as well as peptide transport (transporter 1, TAP1) were significantly up-regulated. Genes for lipid metabolism (hydroxysteroid 11β-dehydrogenase, HSD11B1), prostaglandin metabolism (hydroxyprostaglandin dehydrogenase 15, HPGD15, and prostaglandin E synthase, PTGES) and carbohydrate metabolism (carbonic anhydrase 2 and 12, CA2 and CA12) were also increased in stromal cells. Genes involved in regulation of progression through the cell cycle and regulation of transcription (v-*myc* myelocytomatosis viral oncogene homolog, MYC, and signal transducer and activator of transcription 1, STAT1) were up-regulated.

Many genes that have hitherto been unknown to be expressed in endometrial stromal cells were down-regulated in stromal cells after coculture with trophoblast compared with controls (Table 4). GO grouping of these genes includes many genes for regulation of transcription that is DNA dependent, such as dachshund homolog 1 (DACH1) and sex-determining region Y-box 4 (SOX4) as well as genes responsible for regulation of progression through the cell cycle such as fibroblast growth factor-1 and -9 (FGF-1 and FGF-9) or phospholipase Cβ1 (PLCB1). Furthermore, genes for protein amino acid phosphorylation (dual-specificity tyrosine phosphorylase, DYRK2) and glycosylation (UDP-galactosidase, B3GALT3) were down-regulated between 2- and 6-fold. Many genes for cell adhesion (integrin-α6, ITGA6), signaling transduction (G protein-coupled receptor 153, GPR153), and intracellular signaling cascade (plexin B1, PLXNB1) as well as intracellular protein transport (ADP-ribosylation factor-like 7, ARL7) were also decreased in our experimental setup. Genes with the highest fold change in the decreased group were genes for cytoskeletal anchoring (ankyrin 3, ANK3), for proteolysis (MMP-11; platelet derived

growth factor D, PDGFD; mitochondrial intermediate peptidase, MIPEP; and tripeptidyl peptidase 1, TPP-1), and for humoral immune response (CD24). The most highly down-regulated gene is chondrolectin (CHODL), which is known to be involved in muscle development but has also been shown to be expressed in human testis and was decreased 16.8-fold in our experiment.

Interestingly, there are many GO groups that are both increased and decreased. Instead of just enumerating a list of genes, we also wanted to know how they interact as parts of complex pathways and biological networks. For this purpose, the differentially expressed genes were analyzed using Ingenuity Pathways Analysis software (Ingenuity Systems), and networks as well as individual signaling pathways were generated. The networks describe functional relationship between genes based on known interactions in the literature. Biological functions are assigned to each network, and these networks are then associated with individual canonical pathways. Fourteen highly significant networks with a score of at least 12 were identified from the 284 genes differentially regulated in stromal cells after coculture with trophoblast. First we looked at the network in which our highest regulated gene IL-8 is involved, which was network two. The top functions for this network are labeled inflammatory, immune, hematological, and development and is shown in Fig. 2. IL-15 has direct impact on the expression of genes like IL-8, IL-18 receptor type 1 (IL-18R1), STAT1, and LYN. IL-8, which is most significantly up-regulated in our experiments, is regulated by genes like CXCL1, IL-1 receptor type 1 (IL-1R1), NF-κB inhibitor α (NFKBIA), and MAP3K8. Current literature shows that IL-15 elicits synthesis and release of IL-8 in neutrophils (13) and monocytes (36). Furthermore, IL-15 has the ability to induce NFKB in neutrophils (13). All three of these genes are up-regulated in endometrial stromal cells after coculture with trophoblast. Also IL-1R1, which is the essential receptor for IL-1 signaling (15), induces IL-8 by its activation (see also Fig. 3). In contrast, both CD24 and KIT were down-regulated in our experiments, with CD24 known to be involved in LYN-mediated apoptosis (16) and KIT known to increase proliferation of cells (17).

Figure 3 shows the pathway for IL-6 and IL-8 as it is known to date. Seven of the differentially expressed genes from our data are increased and are shown in red where the symbol IL-1R includes both IL-1 receptor type 1 and IL-1 receptor type 2 (5- and 28-fold increased, respectively). The transcription factor nuclear factor-κB (NF-κB) is increased 2-fold in our data, and NF-κB inhibitor α (IκB) is increased 6-fold. IL-6 signal transducer (IL-6ST, labeled GP130 in Fig. 3) is 2.5-fold increased. IL-8 is the most highly increased gene in our data set (over 300-fold) and TNFAIP6 (TNF α-induced protein 6, labeled TSG6) is increased 4-fold. The figure shows the possible effect of IL-1 produced by the trophoblast acting on endometrial stromal cells through the IL-1R and the NFKB pathway on the induction of IL-8 transcription in the nucleus of endometrial stromal cells.

Validation of gene expression

Real-time PCR was used to validate a selected group of up-regulated and down-regulated genes. The primer sets used are shown in Table 1. IGFBP-1 is already known to play a role in endometrial-trophoblast interaction (18); DKK-1, TIMP-3, MMP-11, and SOX4 have been shown to be regulated in the endometrium during the cycle (19) as well as IL-8 (20, 21), whereas PTX-3 to our knowledge has not been shown in the endometrium to date. All eight genes selected for validation were regulated in PCR as in the microarrays. IL-8, PTX-3, IGFBP-1, DKK-1, and TIMP-3 were up-regulated in a similar fold change both in the microarrays and in real-time PCR experiments (Fig. 4). MMP-11, SOX4, and FGF-1 were all decreased in the same order in the PCR experiments as in the microarray experiments. All but FGF-1 expression changes were statistically significantly regulated in the real-time PCR analysis.

Discussion

High-density DNA microarrays are a powerful tool for the snapshot analysis of the complete gene expression profile of cells and tissues involved in biological processes. In the present study, we used this technology for the analysis of human endometrial stromal cells that have interacted with trophoblast explants in culture mimicking human invasion of trophoblast. Even though we used stromal cells and trophoblast isolated from different individuals, we do not expect an effect on the immune reaction because we know from *in vitro* fertilization cycles with oocyte donations that a similar implantation and pregnancy rate is seen as in blastocysts transferred to their biological mothers. We identified genes that are regulated by this interaction. Our data show tellingly how many different biological processes are regulated concomitantly within stromal cells by contact with trophoblast. The genes identified can be used to further analyze the process of implantation and highlight gene groups involved in stromal cell response to trophoblast invasion.

Of the GOTM categories for up-regulated genes, there is a striking increase of genes involved in immune response and regulation and modulation of inflammatory reaction. Based on published data, all but four of the genes in this GO group have been previously described in endometrium but have not necessarily been associated with trophoblast-stromal interaction. IL-8 has been described to play a role in parturition (22) as well as in the pathogenesis of endometriosis (23). Furthermore, it has been described to be important for the leukocyte recruitment in the endometrium during the secretory phase (24). IL-15 has been demonstrated in first-trimester decidua (25) as well as in nonpregnant endometrium (26) in secretory-phase stromal cells. It is interesting to note that both IL-8 and IL-15 as well as the IL-1 receptor type 1 are up-regulated in the trophoblast coculture as well as in stromal cells treated with progesterone or cAMP (12, 27, 28); however, other cytokines known to be increased in endometrial stromal cells after progesterone or cAMP treatment are not regulated after trophoblast contact, even though progesterone levels in the coculture conditioned medium after 24 h were an average of 35 ng/ml (data not shown). This may reflect inhibitory effects of the trophoblast on cytokine expression. An alternative explanation would be that cytokines or cytokine receptors inhibit production of other cytokines, which would also explain the high redundancy of the cytokine networks. Notably, IL-11 production is regulated by progesterone, estradiol, and relaxin in *in vitro* cultured endometrial stromal cells in both directions (29), showing a complex process of regulation. Our data do not show IL-11 regulation;

TABLE 4. Genes down-regulated in human endometrial stromal cells after trophoblast coculture

Gene symbol	Fold change down	Gene ID	Description
Cell adhesion/cell motility			
ANK3	10.9	206385_s_at	Ankyrin 3, node of Ranvier (ankyrin G)
ADRA2A	8.1	209869_at	Adrenergic, α-2A, receptor
ITGA6	6.1	215177_s_at	Integrin, α6
MYLIP	3.7	220319_s_at	Myosin regulatory light chain interacting protein
CXADR	3.0	203917_at	Coxsackie virus and adenovirus receptor
PCDH7	2.9	205534_at	BH-protocadherin (brain-heart)
ITGB5	2.7	201124_at	Integrin, β5
KIF13B	2.1	202962_at	Kinesin family member 13B
DCHS1	2.0	218892_at	Dachsous 1 (*Drosophila*)
TRO	2.0	211700_s_at	Trophinin
TSPAN6	2.0	209108_at	Tetraspanin 6
Development			
CHODL	16.8	219867_at	Chondrolectin
MPPED2	10.2	205413_at	Metallophosphoesterase domain containing 2
DSCR1L1	5.1	203498_at	Down syndrome critical region gene 1-like 1
PRELP	3.8	204223_at	Proline/arginine-rich end leucine-rich repeat protein
ATRNL1	3.0	213745_at	Attractin-like 1
DPYSL4	2.9	205493_s_at	Dihydropyrimidinase-like 4
PLXNC1	2.7	206470_at	Plexin C1
ANGPTL2	2.6	213001_at	Angiopoietin-like 2
MEST	2.5	202016_at	Mesoderm-specific transcript homolog (mouse)
PBXIP1	2.2	212259_s_at	Pre-B-cell leukemia transcription factor interacting protein 1
PLXNC1	2.0	206471_s_at	Plexin C1
Transcription/replication			
CHES1	2.1	218031_s_at	Checkpoint suppressor 1
DOCK9	2.0	212538_at	Dedicator of cytokinesis 9
Apoptosis/immune response			
CD24	6.4	209772_s_at	CD24 antigen (small cell lung carcinoma cluster 4 antigen)
SOX4	4.7	213668_s_at	SRY (sex determining region Y)-box 4
HDAC5	3.9	202455_at	Histone deacetylase 5
CASP6	2.2	209790_s_at	Caspase 6, apoptosis-related cysteine peptidase
NALP1	2.2	218380_at	NACHT, leucine-rich repeat and PYD (pyrin domain) containing 1
Signal transduction			
DGKI	4.4	206806_at	Diacylglycerol kinase, ι
LPHN3	3.7	209866_s_at	Latrophilin 3
RHOBTB1	3.5	212651_at	Rho-related BTB domain containing 1
ARL7	3.2	202207_at	ADP-ribosylation factor-like 7
PLXNB1	2.9	215807_s_at	Plexin B1
PDE5A	2.8	206757_at	Phosphodiesterase 5A, cGMP-specific
PIK3R3	2.7	202743_at	Phosphoinositide-3-kinase, regulatory subunit 3 (p55, γ)
PLCL3	2.4	214745_at	Phospholipase C-like 3
MYO10	2.4	201976_s_at	Myosin X
WSB1	2.2	201295_s_at	WD repeat and SOCS box-containing 1
HTR2B	2.2	206638_at	5-Hydroxytryptamine (serotonin) receptor 2B
GPR153	2.1	221902_at	G protein-coupled receptor 153
PPAP2A	2.1	209147_s_at	Phosphatidic acid phosphatase type 2A
STMN1	2.0	200783_s_at	Stathmin 1/oncoprotein 18
RALGDS	2.0	209050_s_at	Ral guanine nucleotide dissociation stimulator
Protein metabolism			
EPHA5	6.0	215664_s_at	EPH receptor A5
KIT	4.2	205051_s_at	v-*kit* Hardy-Zuckerman 4 feline sarcoma viral oncogene homolog
TRIB2	3.8	202478_at	Tribbles homolog 2 (*Drosophila*)
EPHA7	3.6	206852_at	EPH receptor A7
KIAA0992	2.4	200906_s_at	Palladin
GAD1	2.3	205278_at	Glutamate decarboxylase 1 (brain, 67 kDa)
B3GALT3	2.3	211379_x_at	UDP-Gal:βGlcNAc β 1,3-galactosyltransferase, polypeptide 3
DAPK1	2.2	203139_at	Death-associated protein kinase 1
TEK	2.1	206702_at	TEK tyrosine kinase, endothelial (venous malformations, multiple cutaneous and mucosal)
DYRK2	2.1	202969_at	Dual-specificity tyrosine-(Y)-phosphorylation regulated kinase 2
NMT2	2.1	205006_s_at	*N*-Myristoyltransferase 2
ST6GAL1	2.0	201998_at	ST6 β-galactosamide α2,6-sialyltransferase 1
Proteolysis			
MMP11	7.7	203876_s_at	Matrix metallopeptidase 11 (stromelysin 3)
MIPEP	2.5	36830_at	Mitochondrial intermediate peptidase
TPP1	2.2	214196_s_at	Tripeptidyl peptidase I

TABLE 4. *Continued*

Gene symbol	Fold change down	Gene ID	Description
Cell cycle/GH			
PDGFD	5.2	219304_s_at	Platelet-derived growth factor D
DUSP6	4.8	206893_s_at	Dual-specificity phosphatase 6
FGF1	4.8	205117_at	Fibroblast growth factor 1 (acidic)
FGF9	4.3	206404_at	Fibroblast growth factor 9 (glia-activating factor)
PLCB1	4.1	213222_at	Phospholipase C, β1 (phosphoinositide-specific)
IGFBP7	2.2	213910_at	IGF-binding protein 7
Transcription/regulation of transcription			
DACH1	8.8	205472_s_at	Dachshund homolog 1 (*Drosophila*)
TOX	6.8	204529_s_at	Thymus high-mobility group box protein TOX
ETV1	6.7	221911_at	*ets* variant gene 1
BACH2	3.3	221234_s_at	BTB and CNC homology 1, basic leucine zipper transcription factor 2
ZNF6	3.2	207781_s_at	Zinc finger protein 6 (CMPX1)
BCL11A	2.9	219497_s_at	B-cell CLL/lymphoma 11A (zinc finger protein)
ZNF365	2.5	206448_at	Zinc finger protein 365
ARFRP2	2.5	219842_at	ADP-ribosylation factor related protein 2
ESR1	2.5	219676_at	ER1
ZNF435	2.5	205225_at	Zinc finger protein 435
TCF4	2.2	212385_at	Transcription factor 4
ZNF84	2.2	204453_at	Zinc finger protein 84 (HPF2)
MAFB	2.2	218559_s_at	v-*maf* Musculoaponeurotic fibrosarcoma oncogene homolog B (avian)
FOXL2	2.1	220102_at	Forkhead box L2
HOXD4	2.1	205522_at	Homeobox D4
ZNF184	2.0	213452_at	Zinc finger protein 184 (Kruppel-like)
Transport			
SLC2A11	4.6	221262_s_at	Solute carrier family 2 (facilitated glucose transporter), member 11
ATP9A	2.5	212062_at	ATPase, Class II, type 9A
SYT11	2.2	209197_at	Synaptotagmin XI
FYCO1	2.1	218204_s_at	FYVE and coiled-coil domain containing 1
Other			
TMEPAI	5.3	217875_s_at	Transmembrane, prostate androgen induced RNA
C5orf13	4.8	201309_x_at	Chromosome 5 open reading frame 13
ASPN	4.4	219087_at	Asporin (LRR class 1)
FLJ12505	4.3	219740_at	Hypothetical protein 12505
LBH	4.2	221011_s_at	Likely ortholog of mouse limb-bud gene
PPP1R3C	4.1	204284_at	Protein phosphatase 1 subunit
FJX1	4.0	219522_at	Four jointed box 1
HSD17B2	3.6	204818_at	Hydroxysteroid 17β-dehydrogenase 2
MYO6	3.6	203215_s_at	Myosin VI
PCOTH	3.5	222277_at	Prostate collagen triple helix
13CDNA73	3.4	204072_s_at	Hypothetical protein CG003
DSPG3	2.9	206439_at	Dermatan sulfate proteoglycan 3
CYFIP2	2.9	215785_s_at	Cytoplasmic FMR 1 interacting protein 2
FNBP1L	2.9	215017_s_at	Formin-binding protein 1-like
DPYSL3	2.8	201431_s_at	Dihydropyrimidinase-like 3
FLJ13197	2.7	219871_at	Hypothetical protein FLJ13197
MYH10	2.6	213067_at	Myosin, heavy polypeptide 10, nonmuscle
ARNT2	2.4	202986_at	Aryl-hydrocarbon receptor nuclear translocator 2
KLHL24	2.4	221986_s_at	Kelch-like 24 (*Drosophilia*)
EFHD1	2.4	209343_at	EF-hand domain family 1
C1orf115	2.4	218546_at	Chromosome 1 open reading frame 115
C21orf91	2.3	220941_s_at	Chromosome 21 open reading frame 91
MGC3032	2.3	210841_at	Hypothetical protein MGC3032
NBEA	2.2	221207_s_at	Neurobeachin
PRPSAP2	2.2	203537_at	Phosphoribosyl pyrophosphate synthetase-associated protein 2
C5orf5	2.1	218518_at	Chromosome 5 open reading frame 5
NDRG4	2.1	209159_s_at	NDRG family member 4
NMT2	2.1	205006_s_at	*N*-Myristoyltransferase 2
C16orf45	2.0	212736_at	Chromosome 16 open reading frame 45
KLHL23	2.0	213610_s_at	Kelch-like 23 (*Drosophila*)
CAMSAP1	2.0	212712_at	Calmodulin-regulated spectrin-associated protein 1
SVEP1	2.0	213247_at	Sushi, vWFA, EGF, pentraxin
IGSF4C	2.0	215259_s_at	Ig superfamily 4
MYST4	2.0	211874_s_at	MYST histone acetyltransferase 4

The fold change is derived from pairwise comparisons of average signal log ratios from three experiments (nine comparisons, at least eight of which had to show a signal log ratio of -1, equivalent to a 2-fold down-regulation).

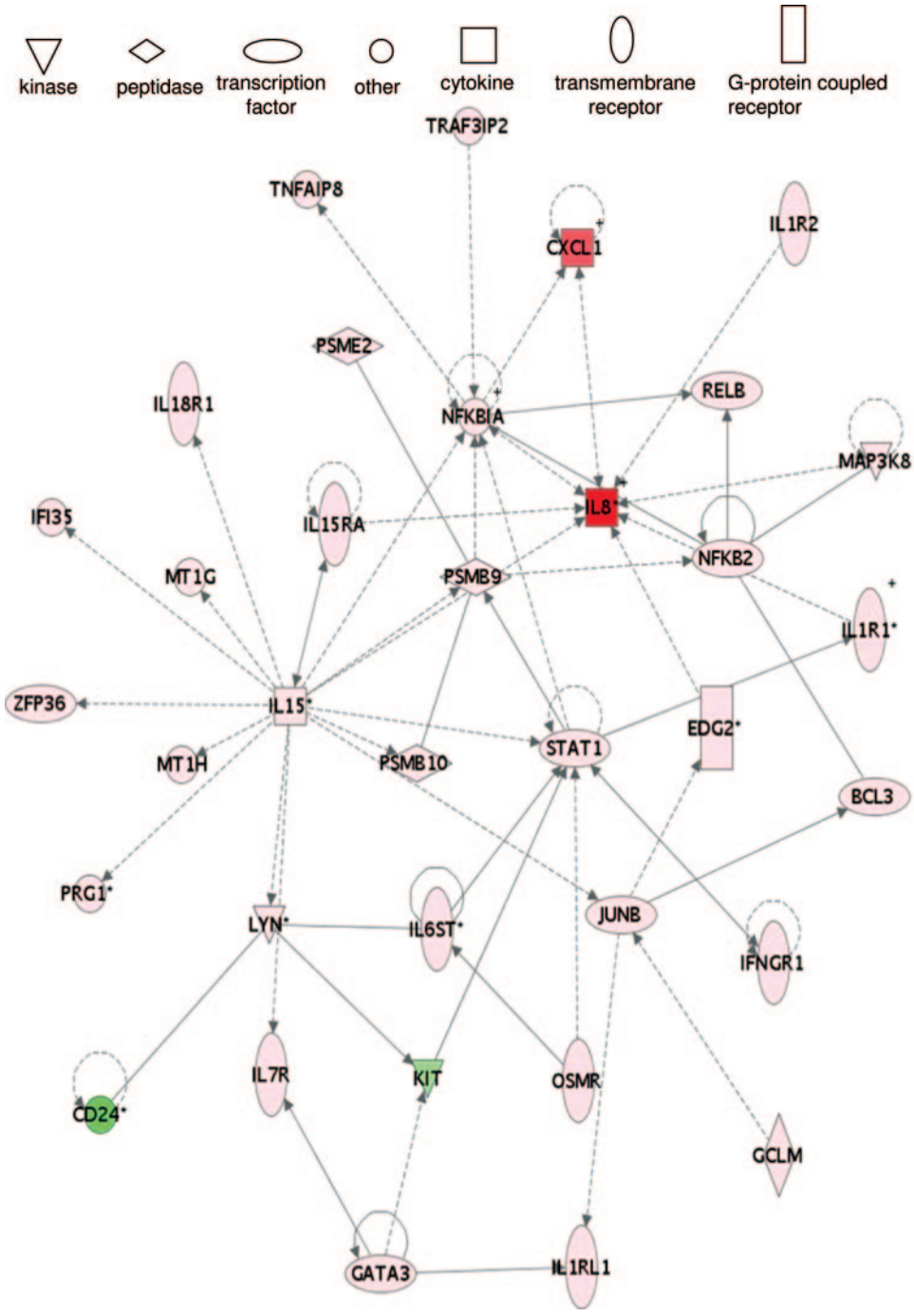

FIG. 2. Functional relationship of factors involved in inflammatory, immune, hematological, and developmental processes during trophoblast interaction with endometrial stromal cells. The intensity of color indicates the degree of up-regulation (*red*) or down-regulation (*green*). Uncommon gene symbols: MT1G, metallothionein 1G; MT1H, metallothionein 1H; EDG2, endothelial differentiation, lysophosphatidic acid G protein-coupled receptor 2; OSMR, oncostation M receptor. IL-15 has direct impact on the expression of genes such as IL-8, IL-18 receptor type 1 (IL-18R1), STAT1, and LYN. IL-8, which is most significantly up-regulated in our experiments, is regulated by genes such as CXCL1, IL-1 receptor type 1 (IL-1R1), NF-κB inhibitor α (NFKBIA), and MAP3K8.

however, gp130 (IL6ST), which is dimerized by binding of IL-11 to its receptor and leads to the activation of the janus kinase/signal transducer and activator of transcription (JAK/STAT) signal transduction pathway (30), is increased 2-fold in our data. Gp130 has hitherto been described in endometrial epithelial cells and is reduced in infertile women (31). Accordingly, STAT1 is increased 2.4-fold and STAT3 1.9-fold. IL-15 is known to be stimulated by progesterone and at the same time is inhibited by IL-1 (32). Both factors are present in our coculture conditioned medium (data not shown). The total effect shown by the data presented herein is an increase of IL-15 expression in endometrial stromal cells because of trophoblast action. Other factors such as IGFBP-1 are even more increased in stromal cells with trophoblast contact than in stromal cells with just progesterone and estrogen treatment (33), which is in accordance with published data showing hCG to further increase IGFBP-1 production in decidualized endometrial stromal cells (34). Our data indicate that a fingerprint gene expression pattern can be shown for trophoblast action on endometrial stromal cells that can be discriminated from progesterone and estradiol action on these cells. Furthermore, our data provide insight on genes that are distinctly changed in their expression by trophoblast action despite both inhibitory and enhancing factors of known origin playing a role. We conclude that the

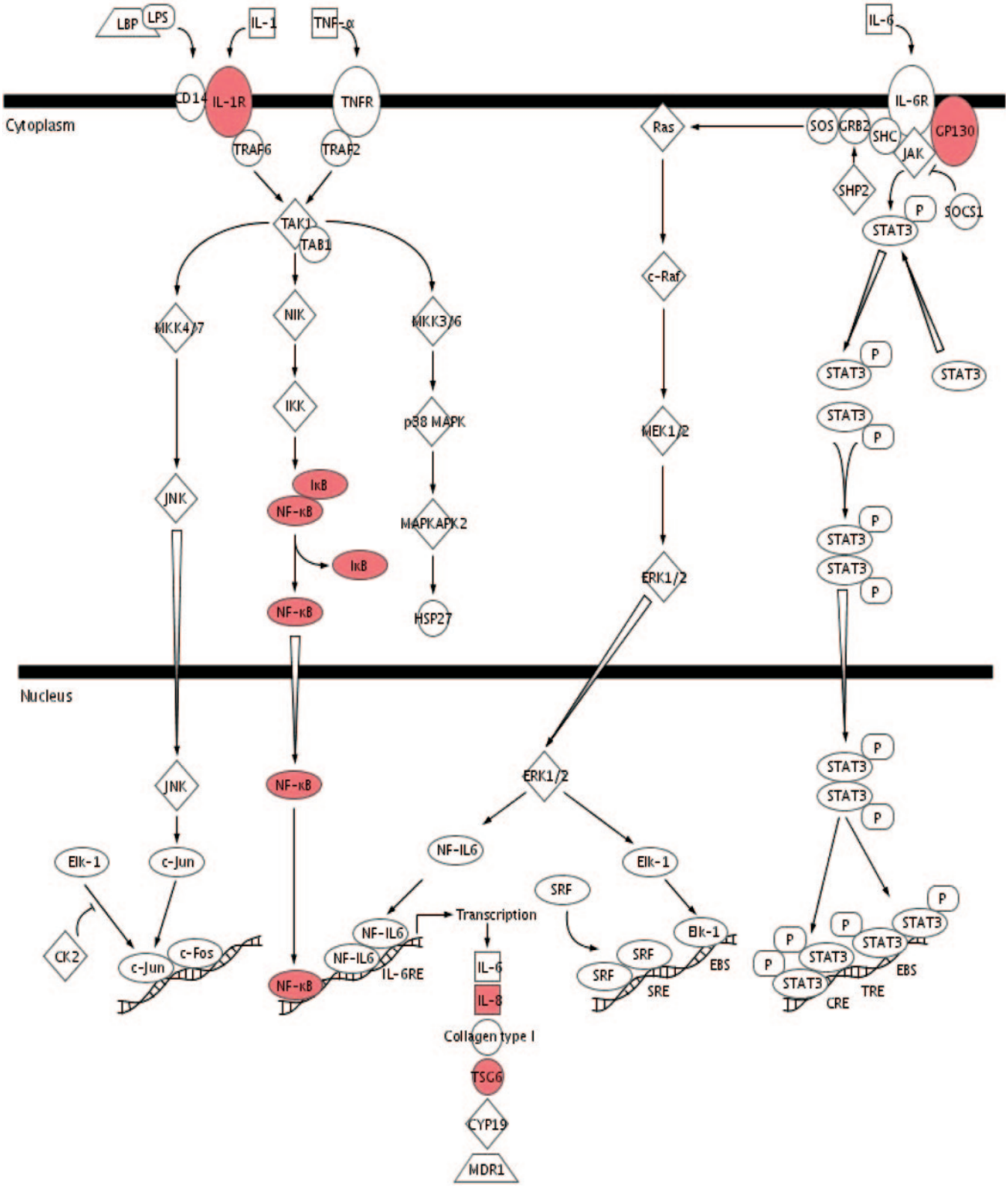

FIG. 3. IL-8 pathway in stromal cells activated by trophoblast. Gene symbols are equivalent to those in Fig. 2. Uncommon gene symbols: IκB, nuclear factor of κ-light polypeptide gene enhancer in B-cells inhibitor α; TSG6, TNF-α-induced protein 6; GP130, IL-6 inducer. The effect of IL-1 produced by the trophoblast acting on endometrial stromal cells through the IL-1R and the NFKB pathway on the induction of IL-8 transcription in the nucleus of endometrial stromal cells is shown.

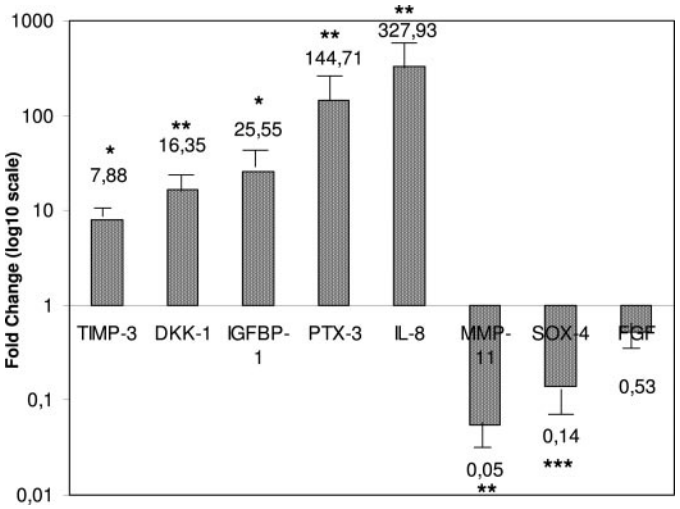

FIG. 4. Validation of microarray data by real-time PCR. Real-time PCR was performed in six experimental samples. Fold change values are displayed above each gene and are blotted on a $\log_{10}$ scale, with P values as follows: *, $P < 0.05$ considered significant; **, $P < 0.01$ highly significant; and ***, $P < 0.001$ extremely highly significant. *Error bars* represent SEM.

trophoblast-induced reaction in stromal cells is a result of multiple factors that have very complex interactions.

This interrelationship can be elucidated on one hand by using both molecular and proteomic systems and on the other hand by using computerized pathway and network building systems, which can help immensely at indicating possible relevant processes, especially for genes not yet described in the endometrium. It is known that IL-8 increases expression of CXCL1 (Gro α) and CXCL2 (Gro β) (35), and simultaneously CXCL1 decreases binding of IL-8 protein (Fig. 3) in the sense of negative regulation. Also, IL-15 induces IL-8 production in human monocytes (36). Pentraxin (PTX3), a gene inducible by TNF-α, IL-β, and lipopolysaccharides, increases CXCL2 production in inflammatory reactions of mice (37). It is very interesting that PTX3 has recently been shown to be elevated in maternal serum of women with preeclampsia and intrauterine growth restriction (38), which are both pathological conditions caused by faulty implantation. Interestingly, in a previous study, human endometrial epithelial cells expressed chemokine receptors CXCR1, CXCR4, and CCR5 when cultured in the presence of a blastocyst in an apposition model for human implantation (39). This shows the importance of the chemokine system for apposition, adhesion, and invasion.

Next to the cytokine system (Fig. 3), additional relevant pathways derived from our data include IGF signaling, PDGF signaling, PPAR signaling and GM-CSF signaling. Common denominators in our study are NFκB signaling, JAK/STAT signaling, and G-protein signaling pathways.

Of further note is the group of genes related to cell death. Many differentially expressed genes belonging to this group are down-regulated in our experiment. Death-associated protein kinase 1 (DAPK1) functions as a positive mediator of apoptosis (40) and is increased by p53 (41) and by TGF-β signal transduction (42). It is reduced 2.2-fold by trophoblast invasion. Histone deacetylase 5 (HDAC 5) is not a p53 target gene, but it also induces apoptosis in multiple tumor cell lines (43). Furthermore, histone deacetylase inhibitors such as suberoylanilide hydroxamic acid (SAHA) or trichostatin A (TSA) induce cell differentiation and are currently tested as anticancer drugs (44). Other genes related to apoptosis are SOX4 and caspase 6. SOX4, a member of the SOX [Sry-related high-mobility group (HMG) box 4] family transcription factors and involved in the determination of cell fate is repressed in stromal cells by trophoblast contact. It may function in the apoptosis pathway leading to cell death (45, 46). In our experiment, a distinct down-regulation of 3.9-fold is notable after trophoblast attachment, which shows an antiapoptotic effect of the trophoblast on endometrial stromal cells. Caspase 6 protein is known to increase apoptosis of different cell types (47). It is processed by caspase 7, 8, and 10 and is thought to function as a downstream enzyme in the caspase activation cascade (48). In rat endometrium, it has been shown to play a key role in apoptosis at estrus, when no embryo has implanted (14), which underscores the importance of its down-regulation when implantation has taken place. In summary, our data suggest that when implantation occurs and trophoblast comes into contact with endometrial stromal cells, a decrease of apoptotic stimulus is required to assure that shedding and destruction of endometrial stroma do not occur. Additionally, antiapoptotic signaling in endometrial stromal cells ensures that stromal cells remain in place and provide a barrier against excessive trophoblast invasion, which could clinically result in placenta accreta. This also supports the finding of increased gene expression of proliferation-related genes such as IGF-II and IGFBP-1, -2, and -4, as well as hepatocyte growth factor (HGF). In summary, we conclude that trophoblast action is inducing proliferation and inhibiting apoptosis in endometrial stromal cells, which is concordant with the implantation-related growth of all uterine structures. At the same time, the down-regulation of cell adhesion molecules between stromal cells (*i.e.* ankyrin) possibly facilitates trophoblast invasion during implantation.

The whole extent of gene expression and interaction cannot entirely be discussed herein; however, additional investigations can be based on the data recruited by this analysis. The extent to which our results can be reproduced *in vivo* remains to be seen, but we hope that they will help future investigation of molecular mechanisms in human implantation and to elucidate predisposing mechanisms to abnormal implantation that result in infertility, recurrent miscarriages, and intrauterine growth restriction as well as preeclampsia.

Acknowledgments

We gratefully thank Dr. Brian Dron and Dr. Adam Corner from Ingenuity Systems, Inc., for their friendly help with the network and pathwork system development. Thanks to all colleagues from the Department of Obstetrics and Gynaecology for support in the collection of tissue samples. Special thanks to Dr. S. Kolay for her constant support during manuscript writing.

Received July 11, 2006. Accepted August 24, 2006.

Address all correspondence and requests for reprints to: Dr. R. M. Popovici, Department of Gynecological Endocrinology and Reproductive Medicine, University of Heidelberg, Voss Strasse 9, 69115 Heidelberg, Germany. E-mail: roxana.popovici@med.uni-heidelberg.de.

Disclosure statement: R.M.P., N.K.B., M.S.K., M.L., J.J., A.G., S.B., A.S., R.K., and M.v.W. have nothing to declare. T.S. received lecture fees from Serono.

References

1. **Kliman HJ, Feinberg RF** 1990 Human trophoblast-extracellular matrix (ECM) interactions in vitro: ECM thickness modulates morphology and proteolytic activity. Proc Natl Acad Sci USA 87:3057–3061
2. **Carver J, Martin K, Spyropoulou I, Barlow D, Sargent I, Mardon H** 2003 An in-vitro model for stromal invasion during implantation of the human blastocyst. Hum Reprod 18:283–290
3. **Campbell S, Rowe J, Jackson CJ, Gallery ED** 2003 In vitro migration of cytotrophoblasts through a decidual endothelial cell monolayer: the role of matrix metalloproteinases. Placenta 24:306–315
4. **Pijnenborg R, Dixon G, Robertson WB, Brosens I** 1980 Trophoblastic invasion of human decidua from 8 to 18 weeks of pregnancy. Placenta 1:3–19
5. **Zhou Y, Fisher SJ, Janatpour M, Genbacev O, Dejana E, Wheelock M, Damsky CH** 1997 Human cytotrophoblasts adopt a vascular phenotype as they differentiate. A strategy for successful endovascular invasion? J Clin Invest 99:2139–2151
6. **Fisher SJ, Damsky CH** 1993 Human cytotrophoblast invasion. Semin Cell Biol 4:183–188
7. **Librach CL, Feigenbaum SL, Bass KE, Cui TY, Verastas N, Sadovsky Y, Quigley JP, French DL, Fisher SJ** 1994 Interleukin-1β regulates human cytotrophoblast metalloproteinase activity and invasion in vitro. J Biol Chem 269:17125–17131
8. **Birkedal-Hansen H** 1993 Role of matrix metalloproteinases in human periodontal diseases. J Periodontol 64(Suppl 5):474–484
9. **Brosens IA, Robertson WB, Dixon HG** 1972 The role of the spiral arteries in the pathogenesis of preeclampsia. Obstet Gynecol Annu 1:177–191
10. **Moodley J, Ramsaroop R** 1989 Placental bed morphology in black women with eclampsia. S Afr Med J 75:376–378
11. **Hustin J, Jauniaux E, Schaaps JP** 1990 Histological study of the materno-embryonic interface in spontaneous abortion. Placenta 11:477–486
12. **Popovici RM, Kao LC, Giudice LC** 2000 Discovery of new inducible genes in *in vitro* decidualized human endometrial stromal cells using microarray technology. Endocrinology 141:3510–3513
13. **McDonald PP, Russo MP, Ferrini S, Cassatella MA** 1998 Interleukin-15 (IL-15) induces NF-κB activation and IL-8 production in human neutrophils. Blood 92:4828–4835
14. **Leblanc V, Dery MC, Shooner C, Asselin E** 2003 Opposite regulation of XIAP and Smac/DIABLO in the rat endometrium in response to 17β-estradiol at estrus. Reprod Biol Endocrinol 1:59
15. **Sims JE, Gayle MA, Slack JL, Alderson MR, Bird TA, Giri JG, Colotta F, Re F, Mantovani A, Shanebeck K** 1993 Interleukin 1 signaling occurs exclusively via the type I receptor. Proc Natl Acad Sci USA 90:6155–6159
16. **Suzuki T, Kiyokawa N, Taguchi T, Sekino T, Katagiri YU, Fujimoto J** 2001 CD24 induces apoptosis in human B cells via the glycolipid-enriched membrane domains/rafts-mediated signalling system. J Immunol 166:5567–5577
17. **Ricotti E, Fagioli F, Garelli E, LInari C, Crescenzio N, Horenstein AL, Pistamiglio P, Vai S, Berger M, di Montezemolo LC, Madon E, Basso G** 1998 c-*kit* Is expressed in soft tissue sarcoma of neuroectodermic origin and its ligand prevents apoptosis of neoplastic cells. Blood 91:2397–2405
18. **Irwin JC, Giudice LC** 1998 Insulin-like growth factor binding protein-1 binds to placental cytotrophoblast $\alpha5\beta1$ integrin and inhibits cytotrophoblast invasion into decidualized endometrial stromal cultures. Growth Horm IGF Res 8:21–31
19. **Talbi S, Hamilton AE, Vo KC, Tulac S, Overgaard MT, Dosiou C, Le Shay N, Nezhat CN, Kempson R, Lessey BA, Nayak NR, Giudice LC** 2006 Molecular phenotyping of human endometrium distinguishes menstrual cycle phases and underlying biological processes in normo-ovulatory women. Endocrinology 147:1097–1121
20. **Arici A, Seli E, Senturk LM, Gutierrez LS, Oral E, Taylor HS** 1998 Interleukin-8 in the human endometrium. J Clin Endocrinol Metab 83:1783–1787
21. **von Wolff M, Thaler CJ, Strowitzki T, Broome J, Stolz W, Tabibzadeh S** 2000 Regulated expression of cytokines in human endometrium throughout the menstrual cycle: dysregulation in habitual abortion. Mol Hum Reprod 6:627–634
22. **Kelly RW, Leask R, Calder AA** 1992 Choriodecidual production of interleukin-8 and mechanism of parturition. Lancet 339:776–777
23. **Ulukus EC, Ulukus M, Seval Y, Zheng W, Arici A** 2005 Expression of interleukin-8 and monocyte chemotactic protein-1 in adenomyosis. Hum Reprod 20:2958–2963
24. **Jones RL, Hannan NJ, Kaitu'u TJ, Zhang J, Salamonsen LA** 2004 Identification of chemokines important for leukocyte recruitment to the human endometrium at the times of embryo implantation and menstruation. J Clin Endocrinol Metab 89:6155–6167
25. **Kitaya K, Yasuda J, Yagi I, Tada Y, Fushiki S, Honjo H** 2000 IL-15 expression at human endometrium and decidua. Biol Reprod 63:683–687
26. **Okada S, Okada H, Sanezumi M, Nakajima T, Yasuda K, Kanzaki** H 2000 Expression of interleukin-15 in human endometrium and decidua. Mol Hum Reprod 6:75–80
27. **Dunn CL, Critchley HO, Kelly RW** 2002 IL-15 regulation in human endometrial stromal cells. J Clin Endocrinol Metab 87:1898–1901
28. **Okada H, Nakajima T, Sanezumi M, Ikuta A, Yasuda K, Kanzaki H** 2000 Progesterone enhances interleukin-15 production in human endometrial stromal cells *in vitro*. J Clin Endocrinol Metab 85:4765–4770
29. **Dimitriadis E, White CA, Jones RL, Salamonsen LA** 2005 Cytokines, chemokines and growth factors in endometrium related to implantation. Hum Reprod Update 11:613–630
30. **Heinrich PC, Behrmann I, Muller-Newen G, Schaper F, Graeve L** 1998 Interleukin-6-type cytokine signalling through the gp130/Jak/STATpathway. Biochem J 334:297–314
31. **Sherwin JR, Smith SK, Wilson A, Sharkey AM** 2002 Soluble gp130 is up-regulated in the implantation window and shows altered secretion in patients with primary unexplained infertility. J Clin Endocrinol Metab 87:3953–3960
32. **Okada H, Nakajima T, Yasuda K, Kanzaki H** 2004 Interleukin-1 inhibits interleukin-15 production by progesterone during in vitro decidualization in human. J Reprod Immunol 61:3–12
33. **Popovici RM, Lu M, Bhatia S, Faessen GH, Giaccia AJ, Giudice LC** 2001 Hypoxia regulates insulin-like growth factor-binding protein 1 in human fetal hepatocytes in primary culture: suggestive molecular mechanisms for *in utero* fetal growth restriction caused by uteroplacental insufficiency. J Clin Endocrinol Metab 86:2653–2659
34. **Licht P, Russu V, Wildt L** 2001 On the role of human chorionic gonadotropin (hCG) in the embryo-endometrial microenvironment: implications for differentiation and implantation. Semin Reprod Med 19:37–47
35. **Smith DF, Galkina E, Ley K, Huo Y** 2005 GRO family chemokines are specialized for monocyte arrest from flow. Am J Physiol Heart Circ Physiol 289:1976–1984
36. **Badolato R, Ponzi AN, Millesimo M, Notarangelo LD, Musso T** 1997 Interleukin-15 (IL-15) induces IL-8 and monocyte chemotactic protein 1 production in human monocytes. Blood 90:2804–2809
37. **Souza DG, Soares AC, Pinho V, Torloni H, Reis LF, Martins MT, Dias AA** 2002 Increased mortality and inflammation in tumor necrosis factor-stimulated gene-14 transgenic mice after ischemia and reperfusion injury. Am J Pathol 160:1755–1765
38. **Cetin I, Cozzi V, Pasqualini F, Nebuloni M, Garlanda C, Vago L, Pardi G, Mantovani A** 2006 Elevated maternal levels of the long pentraxin 3 (PTX3) in preeclampsia and intrauterine growth restriction. Am J Obstet Gynecol 194: 1347–1353
39. **Dominguez F, Galan A, Martin JJL, Remohi J, Pellicer A, Simon C** 2003 Hormonal and embryonic regulation of chemokine receptors CXCR1, CXCR4, CCR5 and CCR2B in the human endometrium and the human blastocyst. Mol Hum Reprod 9:189–198
40. **Lee JH, Rho SB, Chun T** 2005 Programmed cell death 6 (PDCD6) protein interacts with death-associated protein kinase 1 (DAPk1): additive effect on apoptosis via caspase-3 dependent pathway. Biotechnol Lett 27:1011–1015
41. **Martoriati A, Doumont G, Alcalay M, Bellefroid E, Pelicci PG, Marine JC** 2005 dapk1, encoding an activator of a p19ARF-p53-mediated apoptotic checkpoint, is a transcription target of p53. Oncogene 24:1461–1466
42. **Dairkee SH, Ji Y, Ben Y, Moore DH, Meng Z, Jeffrey SS** 2004 A molecular 'signature' of primary breast cancer cultures; patterns resembling tumor tissue. BMC Genomics 5:47
43. **Huang Y, Tan M, Gosink M, Wang KK, Sun Y** 2002 Histone deacetylase 5 is not a p53 target gene, but its overexpression inhibits tumor cell growth and induces apoptosis. Cancer Res 62:2913–2922
44. **Uchida H, Maruyama T, Nagashima T, Asada H, Yoshimura Y** 2005 Histone deacetylase inhibitors induce differentiation of human endometrial adenocarcinoma cells through up-regulation of glycodelin. Endocrinology 146:5365–5373
45. **Ahn SG, Kim HS, Jeong SW, Kim BE, Rhim H, Shim JY, Kim JW, Lee JH, Kim IK** 2002 Sox-4 is a positive regulator of Hep3B and HepG2 cells' apoptosis induced by prostaglandin (PG)A_2 and δ_{12}-PGJ_2. Exp Mol Med 34:243–249
46. **Pramoonjago P, Baras AS, Moskaluk CA** 2006 Knockdown of Sox4 expression by RNAi induces apoptosis in ACC3 cells. Oncogene 25:5626–5639
47. **Nagata S** 1997 Apoptosis by death factor. Cell 88:355–365 (Review)
48. **Kawahara A, Enari M, Talanian RV, Wong WW, Nagata S** 1998 Fas-induced DNA fragmentation and proteolysis of nuclear proteins. Genes Cells 3:297–306 (Review)

***Endocrinology* is published monthly by The Endocrine Society (http://www.endo-society.org), the foremost professional society serving the endocrine community.**